J.Natn.Sci.Foundation Sri Lanka 2023 51 (2): 373 - 385
DOI: http://dx.doi.org/10.4038/jnsfsr.v51i2.10777

RESEARCH ARTICLE

Mathematical Modelling

Comparative analysis of three memory selection methods for time integration of Fractional Reaction-Diffusion Equations

LW Somathilake

Department of Mathematics, Faculty of Science, University of Ruhuna, Matara, Sri Lanka.

Submitted: 08 November 2021; Revised: 30 September 2022; Accepted: 28 October 2022

Abstract: By discretising in space, non-linear time fractional reaction-diffusion equations(TFRDEs) can be converted into a system of time-fractional differential equations (TFDEs). The full memory method (FMM) and short memory method (SMM) are well-established memory selection methods used in the time integration of TFDEs. The main drawbacks of FMM and SMM are higher computational cost and uncontrollable error respectively. The only way to increase the accuracy of SMM is by increasing short memory length which causes an increase in computational cost. Especially when we apply these two methods to integrate TFRDEs, we have to solve a large system of TFDEs. Therefore, the drawbacks of these two methods affect seriously, when these are applied to solve TFRDEs. This paper aims to investigate the accuracy and efficiency of the memory selection method, Exponentially Decreasing Random Memory Method (EDRMM), and compare it with FMM and SMM when these methods apply to integrate TFRDEs. Based on these three memory selection methods, three semi-implicit numerical schemes namely semi-implicit scheme with full memory method (SI-FMM), semi-implicit scheme with short memory method (SI-SMM), and semi-implicit scheme with exponentially decreasing random memory method (SI-EDRMM)) are proposed and the accuracy and CPU time (computational time (CT)) of these three numerical schemes are compared. To do this comparison, these three numerical schemes are applied to four TFRDEs whose exact solutions are known. Numerical experiments confirm that the accuracy and efficiency of the SI-EDRMM are better than that of SI-SMM and the efficiency of SI-EDRMM is higher than that of SI-FMM. Therefore, EDRMM is better than SMM and FMM for the integration of TFRDEs.

Keywords: Fractional differential equations, Full memory method, Short memory method, Time fractional reaction-diffusion equations.

INTRODUCTION

Fractional order models can be more appropriate than standard order (with integer-order derivatives and integrals) models as fractional derivatives and integrals bring forwards the temporal and spatial memory heredity of materials and processes. This is the main advantage of fractional-order models when compared to those with integer-order models. In a usual reaction-diffusion equation, both time derivative and spacial derivative (diffusion term) are integer order. This paper considers reaction-diffusion equations with fractional order time derivatives and integral order diffusion terms. This type of models are called time fractional reaction-diffusion equations (TFRDEs). There

* Corresponding author (lwsoma@gmail.com; https://orcid.org/0000-0002-7276-1357)

is no unique definition for the fractional derivative. Caputo fractional derivative and Riemann-Liouville derivative are the more well-known fractional derivatives. In this paper, Caputo fractional derivative is applied to solve TFRDEs. Throughout this paper $\lceil x \rceil$ denotes the smallest integer greater than the real number x.

Definition 1 (Caputo derivative Podlubny & Igor (1999))**.** *The Caputo fractional derivative of order γ of $u(t)$ is defined as*

$$ {}_a^C D_t^{\gamma} u(t) = \begin{cases} \dfrac{1}{\Gamma(n-\gamma)} \displaystyle\int_a^t (t-\tau)^{n-\gamma-1} \frac{d^n u(\tau)}{d\tau^n} d\tau, & n-1 < \gamma < n, \\ \dfrac{d^n u(t)}{dt^n}, & \gamma = n, \end{cases} \tag{1} $$

where, $\Gamma(z)$ $(z \in \mathbb{C})$ denotes the Euler Gamma function defined by $\Gamma(z) = \displaystyle\int_0^{\infty} x^{z-1} e^{-x} dx$, γ is the order of the derivative, $n = \lceil \gamma \rceil \in \mathbb{N}$, $a \in \mathbb{R}$ is the initial time.

In this paper time fractional reaction diffusion equations (TFRDEs) of the following form are considered with suitable initial and boundary conditions.

$$ \frac{\partial^{\gamma} u(x,t)}{\partial t^{\gamma}} = d\Delta u(x,t) + F(u(x,t),x,t), \quad x \in \bar{\Omega} \subset \mathbb{R}^l, \quad 0 < \gamma \leq 1, \quad 0 \leq t \leq T. \tag{2} $$

Here, $\gamma, d, T \in \mathbb{R}$, $l \in \mathbb{N}$, and the fractional differential operator is in the sense of Caputo derivative. Since $0 < \gamma < 1$, in order to solve this type of TFRDEs uniquely, one initial condition and boundary conditions are required. In physical applications, meanings of the fractional-order derivatives are unknown, but physical meanings of the integer-order derivatives are known. Therefore, in physical applications, implementing the Riemann-Liouville derivative is inappropriate as fractional order derivatives of initial conditions are necessary to implement this derivative. However, it is possible to implement fractional-order Caputo derivative in physical applications as just integer-order derivatives of initial conditions are sufficient in this derivative, and the physical meanings of these derivatives are known. Therefore, in this paper, fractional-order Caputo derivative is applied in constructing numerical schemes.

Basic theoretical aspects of fractional order differential equations have been reported by Podlubny & Igor (1999), Lakshmikantham & Vatsala (2008), Zhou *et al.* (2012), El-Sayed & El-Maghrabi (2008), and Caballero *et al.* (2011). Different types of instabilities in time fractional reaction-diffusion systems are reported by Gafiychuk & Datsko (2010). Approximate analytical solutions of some fractional reaction-diffusion equations are presented by Khan *et al.* (2012). A method to find numerical solutions of space fractional reaction-diffusion equations, based on operator splitting method, is proposed by Baeumer *et al.* (2008).

Adams type predictor-corrector method for numerical solutions of fractional differential equations is discussed by Diethelm *et al.* (2002). The author Deng (2007), has used a predictor-corrector approach where the short memory principle is applied to solve fractional differential equations. A numerical scheme for fractional differential equations based on Grünwald-Letnikov fractional-order derivative has been discussed by Scherer, Kalla, Tang & Huang (Scherer *et al.)*. In that paper stability, convergence, and error propagation of the numerical scheme are discussed. The short memory principle has been applied for solving fractional order Abel differential equation by Xu & He (2011). Stability properties and order of convergence of some numerical schemes for TFDEs have been explained by Deng & Li (2012). The fast predictor-corrector method has been applied for fractional differential equations by Deng *et al.* (2016).

An implicit difference approximation for TFRDEs has been explained by Zhuang & Liu (2006). The author Rida *et al.* (2010) hs used the generalized differential transform method to solve TFRDEs. Finite difference approaches have been applied to simulate TFRDEs by Murio (2008), and Zheng *et al.* (2017). In these works, full memory has been considered and it causes high computational cost. Reducing computational cost by controlling numerical errors is the main challenge in the integration of TFRDEs. This paper aims to investigate the effectiveness of the exponentially decreasing random memory method (Somathilake (2020)) in solving TFRDEs.

MATERIAL AND METHODS

In order to integrate TFRDEs of the form (2), at first it is transformed into a system of TFDEs by discretising in space.

Space discretisation

By discretising in space, the time fractional reaction-diffusion equation (2) can be approximated to a system of ODEs of the form

$$\frac{d^{\gamma}\mathbf{u}}{dt^{\gamma}} = -\frac{1}{h^2}A\mathbf{u} + \mathbf{F}(\mathbf{u},\mathbf{x},t), \quad t \in [0,T], \quad \mathbf{u}(0) = \mathbf{u}^0, \tag{3}$$

on finite time interval $[0,T]$. The vectors $\mathbf{x}$, $\mathbf{u}$ and $\mathbf{F}$ represent the spatial discretisations of x, u and F respectively, and A is the discrete Laplacian operator coupled with relevant boundary conditions. For example, the discrete Laplacian operator, A, on $[0,L_1]$, obtained with a finite difference approximation on a uniform mesh of n_1+1 nodes with step size $h = L_1/n_1$ is given by

$$A = \begin{pmatrix} 1 & -1 & & & \\ -1 & 2 & -1 & & \\ & \ddots & \ddots & \ddots & \\ & & -1 & 2 & -1 \\ & & & -1 & 1 \end{pmatrix}_{(n_1+1)\times(n_1+1)}, \text{ and } A = \begin{pmatrix} 2 & -1 & & & \\ -1 & 2 & -1 & & \\ & \ddots & \ddots & \ddots & \\ & & -1 & 2 & -1 \\ & & & -1 & 2 \end{pmatrix}_{(n_1-1)\times(n_1-1)}.$$

subject to homogeneous Neumann boundary conditions and Dirichlet boundary conditions respectively. The discrete Laplacian in higher dimensions can be obtained by taking Kronecker (tensor) products of respective one-dimension discrete Laplacian embedding boundary conditions.

Constructed systems of ODEs are solved using numerical schemes explained in the next section and these numerical schemes are compared.

Numerical implementation of Caputo derivative with full memory

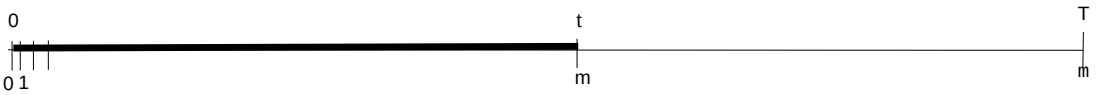

Figure 1: Sketch for the selection of full memory length

Discretising the time fractional Caputo derivative of order γ $(0 < \gamma < 1)$ using finite difference formula Karatay *et al.* (2011), we get

$${}_{FM}D^{\gamma}_{0,t}\mathbf{u}(t_m) = \frac{1}{(\Delta t)^{\gamma}} \sum_{k=0}^{m} g_k^{\gamma}(\mathbf{U}^{m-k} - \mathbf{U}^0), \tag{4}$$

where $\mathbf{U}^k$ denotes the numerical approximation to the exact value $\mathbf{u}(t)$ at $t = t_m = m\Delta t$. Here, $g_k^{\gamma} = (-1)^k \begin{pmatrix} \gamma \\ k \end{pmatrix}$ where $\begin{pmatrix} \gamma \\ k \end{pmatrix} = \dfrac{\Gamma(\gamma+1)}{k!\Gamma(\gamma-k+1)}$ represents the fractional binomial coefficients. Also, g_k^{γ} satisfies the recursive relation $g_0^{\gamma} = 1$, $g_k^{\gamma} = \left(1 - \dfrac{\gamma+1}{k}\right) g_{k-1}^{\gamma}$ for $k > 1$.

Numerical implementation of Caputo derivative with fixed (short) memory length

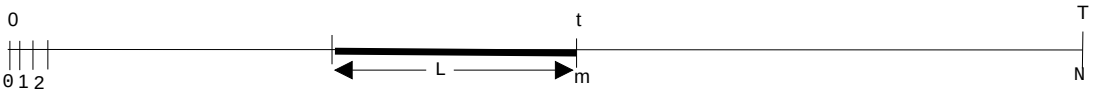

Figure 2: Sketch for the selection of short memory length

Definition 2. *Let $0 < \gamma < 1$, $L \geq 0$, and $u(t)$ an integrable function in the interval $[t-L,t]$. Then the fractional derivative with fixed (short) memory length L of $u(t)$, ${}_{SM}D^{\gamma}_{0,t}\mathbf{u}(t)$, can be defined (base on Abdelouahab & Hamri (2016)) as*

$$ {}_{SM}D^{\gamma}_{0,t}\mathbf{u}(t_m) = \begin{cases} \dfrac{1}{(\Delta t)^{\gamma}} \displaystyle\sum_{k=0}^{\lceil L/\Delta t \rceil} g_k^{\gamma} \left(\mathbf{U}^{m-k} - \mathbf{U}^0\right), & \text{if } t_m > L, \\ \dfrac{1}{(\Delta t)^{\gamma}} \displaystyle\sum_{k=0}^{m} g_k^{\gamma} \left(\mathbf{U}^{m-k} - \mathbf{U}^0\right), & \text{if } t_m \leq L. \end{cases} \tag{5} $$

Numerical implementation of Caputo derivative with exponentially decreasing random memory

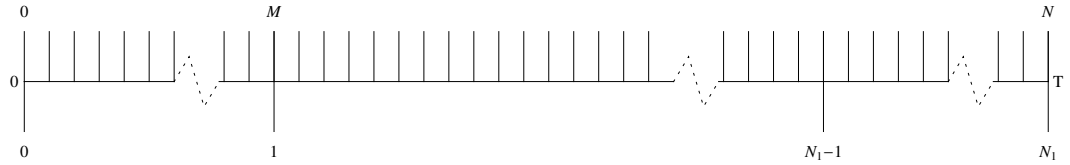

Figure 3: Sketch for the discretisation of the time interval $[0,T]$.

A discrete fractional order derivative on uniform meshes choosing memory points randomly and exponentially decreasing along the tail of the memory is introduced by Somathilake (2020). We called this method the exponentially decreasing random Memory method (EDRMM). In the derivation of this method the full-time interval $[0,T]$ is discretised into N number of partitions with equal step size Δt. M and N_1 are integers such that $N_1 = N/M$ (see Figure 3). That is the interval $[0,T]$ is divided into N_1 number of partitions P_1, P_2,...,P_{N_1} with equal length $M\Delta t$. The fractional order derivative with exponentially decreasing random memory is defined as follows (please see Somathilake (2020)).

$$ {}_{RM}D^{\gamma}_{0,t}u(t_m) = \begin{cases} \dfrac{1}{(\Delta t)^{\gamma}} \displaystyle\sum_{k=0}^{m} g_k^{\gamma} \left(U^{(m-k)} - U^0\right), & m < 2M, \\ \dfrac{1}{(\Delta t)^{\gamma}} \left(\displaystyle\sum_{k=0}^{n_2} g_k^{\gamma} \left(U^{(m-k)} - U^0\right) + \sum_{j=1}^{n_1-1} w_j \sum_{i=1}^{R_j} g_{l_{i,j}}^{\gamma} \left(U^{(m-l_{i,j})} - U^0\right) \right), & m \geq 2M. \end{cases} \tag{6} $$

Here, $t = m\Delta t$, $n_1 = \lceil \dfrac{m}{N} \rceil - 1$, $n_2 = m - M(n_1 - 1)$ if $n_1 \geq 2$, $R_j = \left\lceil Me^{(-\alpha j/N_1)} \right\rceil$; $w_j = M/R_j$ for $j = 1,2,...,n_1-1$, $l_{i,j} = n_2 + (j-1)M + a_i^j$. Also, α is a real number that determines the decreasing speed of the number of memory points from the partition P_i to P_{i+1} for $i = 1,2,...,n_1-1$ and $\{a_1^i, a_2^i, ..., a_{R_i}^i\}$ is a set of R_i number of random integers chosen in the i^{th} partition P_i ($i = 1,2,...,N_1$).

Numerical methods

This section introduces three semi-implicit numerical schemes based on the fractional order derivatives described in the previous section.

A semi-implicit scheme with full memory method (SI-FMM)

Replacing the fractional derivative of order γ of (3), by the finite difference formula (4) we get

$$\frac{1}{(\Delta t)^\gamma}\sum_{k=0}^{m} g_k^\gamma(\mathbf{U}^{(m-k)}-\mathbf{U}^0) \quad = \quad -\frac{1}{h^2}A\mathbf{U}^m+\mathbf{F}^{m-1}, \quad m=1,2,...N, \tag{7}$$

where $\mathbf{U}^m=\mathbf{U}(\mathbf{x},t^m)$, $\mathbf{F}^m=\mathbf{F}(\mathbf{U}^m,\mathbf{x},t^m)$, $t^m=m\Delta t$. Rearranging the system (7) we get a semi-implicit scheme:

$$\left(I+\frac{(\Delta t)^\gamma}{h^2}A\right)\mathbf{U}^m \quad = \quad \mathbf{U}^0-\sum_{k=1}^{m} g_k^\gamma\left(\mathbf{U}^{(m-k)}-\mathbf{U}^0\right)+(\Delta t)^\gamma\mathbf{F}^{m-1}, \quad m=1,2,...N. \tag{8}$$

In the summation at the right hand at the m^{th} time step, m number of vector summations has to be done.

A semi-implicit scheme with short memory method (SI-SMM)

By replacing the fractional derivative of order γ of (3), by the finite difference formulas (5) and rearranging terms we obtained the following semi-implicit numerical scheme.

$$\left(I+\frac{(\Delta t)^\gamma}{h^2}A\right)\mathbf{U}^m=\begin{cases}\mathbf{U}^0-\sum_{k=1}^{m} g_k^\gamma\left(\mathbf{U}^{(m-k)}-\mathbf{U}^0\right)+(\Delta t)^\gamma\mathbf{F}^{m-1}, & \text{if } m\le N_L,\\ \mathbf{U}^0-\sum_{k=1}^{N_L} g_k^\gamma\left(\mathbf{U}^{(m-k)}-\mathbf{U}^0\right)+(\Delta t)^\gamma\mathbf{F}^{m-1}, & \text{if } m>N_L,\end{cases} \tag{9}$$

for $m=1,2,...N$. Here, $N_L=\lceil L/\Delta t\rceil$.

A semi-implicit scheme with exponentially decreasing random memory method (SI-EDRMM)

By replacing the fractional derivative of order γ of (3), by the finite difference formulas (6) and rearranging the terms we obtain following numerical scheme.

$$\left(I+\frac{(\Delta t)^\gamma}{h^2}A\right)\mathbf{U}^m=\begin{cases}\mathbf{U}^0-\sum_{k=1}^{m} g_k^\gamma\left(\mathbf{U}^{(m-k)}-\mathbf{U}^0\right)+(\Delta t)^\gamma\mathbf{F}^{m-1}; & \text{if } m<2M,\\ \mathbf{U}^0-B+(\Delta t)^\gamma\mathbf{F}^{m-1}; & \text{if } m\ge 2M,\end{cases} \tag{10}$$

where $B=\sum_{k=1}^{n_2} g_k^\gamma\left(\mathbf{U}^{(m-k)}-\mathbf{U}^0\right)+\sum_{j=1}^{n_1-1} w_j\sum_{i=1}^{R_j} g_{l_{i,j}}^\gamma\left(\mathbf{U}^{(m-l_{i,j})}-\mathbf{U}^0\right)$.

RESULTS AND DISCUSSION

Numerical experiments

Three TFRDEs in one dimension and one TFRDE in two dimensions of the form (2) are considered for the numerical experiments. These TFRDEs were converted into a system of TFDEs of the form (3) by discretising in space and solved using numerical schemes as explained in the above section. Algorithms for these numerical schemes were implemented and solved using Matlab on a 2.3GHz, Intel Core i5 laptop computer that had 8GB of RAM and Microsoft Windows 10. In this section, we demonstrate the accuracies and computational cost of the numerical schemes discussed in section based on the numerical solutions of these three TFRDEs.

TFRDE 1 (in one dimension): The first TFRDE is

$$\left.\begin{aligned} &\frac{\partial^\gamma u(x,t)}{\partial t^\gamma} = \frac{\partial^2 u(x,t)}{\partial x^2} + F(x,t), \quad (0<x<1,\ \ 0<t<T,\ \ T>0),\\ &u(x,0) = 0, \quad 0 \le x \le 1,\\ &u(0,t) = t^2, \quad u(1,t) = t^2 e, \quad 0 \le t \le T, \end{aligned}\right\}. \tag{11}$$

Here $F(x,t) = t^2\left(\dfrac{2e^x t^{-\gamma}}{\Gamma(3-\gamma)} - 1\right)$. The exact solution of this fractional reaction-diffusion equation is $u(x,t) = t^2 e^x$.

TFRDE 2 (in one dimension): The second TFRDE is

$$\left.\begin{aligned} &\frac{\partial^\gamma u(x,t)}{\partial t^\gamma} = \frac{\partial^2 u(x,t)}{\partial x^2} + G(x,t), \quad (0<x<1,\ \ 0<t<T,\ \ T>0),\\ &u(x,0) = 10x^2(1-x), \quad 0 \le x \le 1,\\ &u(0,t) = u(1,t) = 0.0, \quad 0 \le t \le T, \end{aligned}\right\}. \tag{12}$$

Here $G(x,t) = 10x^2(1-x)\left(\dfrac{t^{2-\gamma}}{\Gamma(3-\gamma)} + \dfrac{t^{1-\gamma}}{\Gamma(2-\gamma)}\right) - 20(t+1)^2(1-3x)$.
The exact solution of this time fractional reaction-diffusion equation is
$u(x,t) = 10x^2(1-x)(1+t)^2$.

TFRDE 3 (in one dimension): Considered third TFRDE is

$$\left.\begin{aligned} &\frac{\partial^\gamma u(x,t)}{\partial t^\gamma} = \frac{\partial^2 u(x,t)}{\partial x^2} + F(u) + G(x,t), \quad (0<x<1,\ \ 0<t<T,\ \ T>0),\\ &u(x,0) = 0.0, \quad 0 \le x \le 1,\\ &u(0,t) = 0.0, \quad u(1,t) = t, \quad 0 \le t \le T, \end{aligned}\right\}. \tag{13}$$

Here $F(u) = u(1-u)$, $G(x,t) = \dfrac{x^2 t^{1-\gamma}}{\Gamma(2-\gamma)} - x^2 t(1-x^2 t) - 2t$.
The exact solution of this time fractional reaction-diffusion equation is $u(x,t) = x^2 t$.

TFRDE 4 (in two dimensions): The time-fractional diffusion equation (11) in two dimension is:

$$\left.\begin{aligned} &\frac{\partial^\gamma u(x,y,t)}{\partial t^\gamma} = \frac{\partial^2 u(x,y,t)}{\partial x^2} + \frac{\partial^2 u(x,y,t)}{\partial y^2} + t^2\left(\frac{2t^{-\gamma}e^{x+y}}{\Gamma(3-\gamma)} - 1\right),\\ &u(x,y,0) = 0, \quad u(x,0,t) = e^x t^2, \quad u(0,x,t) = e^y t^2,\\ &u(x,1,t) = e^{1+x} t^2, \quad u(1,y,t) = e^{1+y} t^2, \end{aligned}\right\}. \tag{14}$$

Here, $0 < x,y < 1$, $0 < t < T$, $T > 0$. The exact solution of this time fractional reaction-diffusion equation is $u(x,y,t) = t^2 e^{x+y}$.

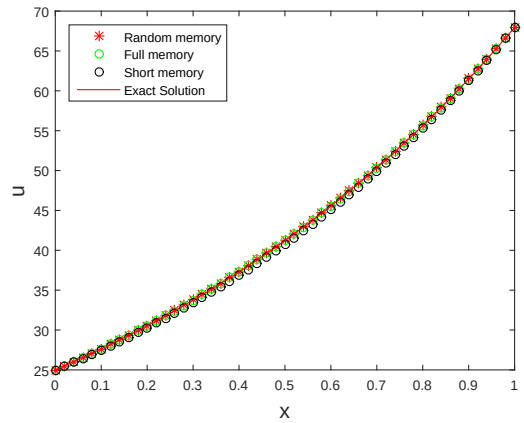

(a) Solutions of (11).

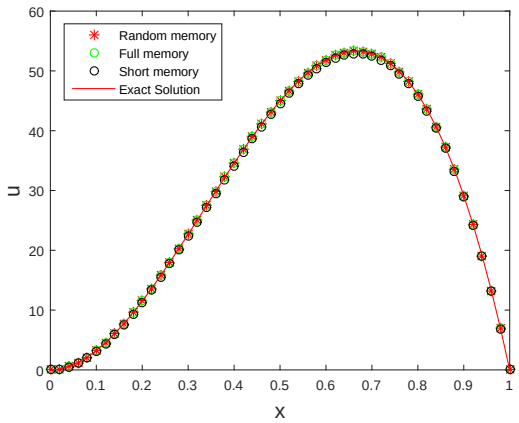

(b) Solutions of (12).

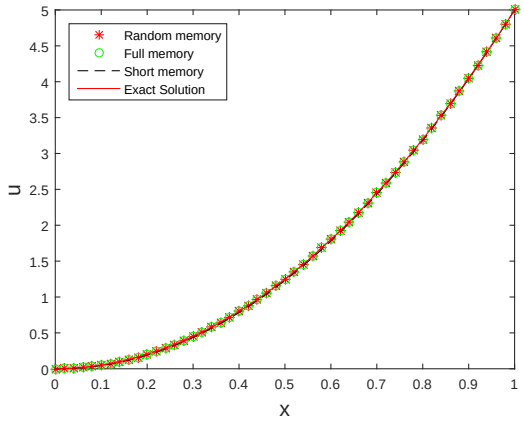

(c) Solutions of (13).

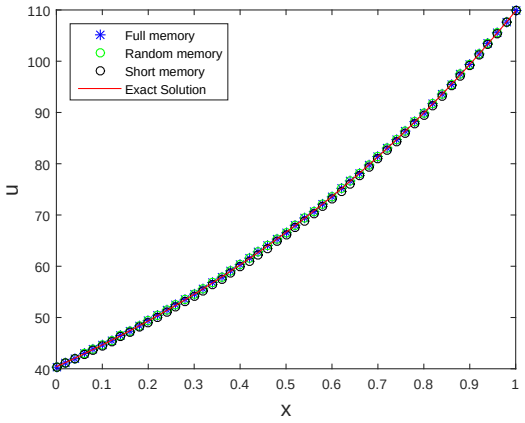

(d) Solutions of (14).

Figure 4: Exact solutions and numerical solutions of the time fractional reaction-diffusion equations (11)-(14) at $t = 5$ for the range $0 \leq x \leq 1$. Solution of (14) is evaluated at $y = 0.5$.

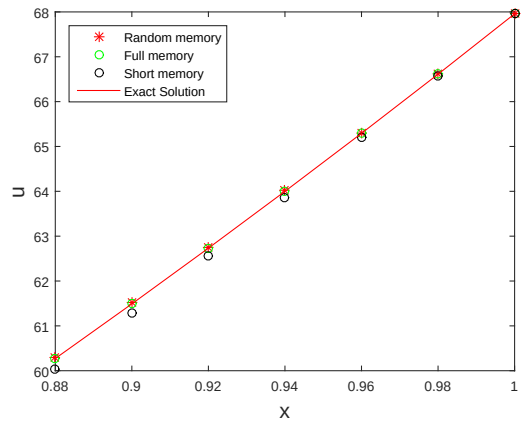

(a) Solutions of (11) at $t = 5$ for $0.88 \leq x \leq 1.0$.

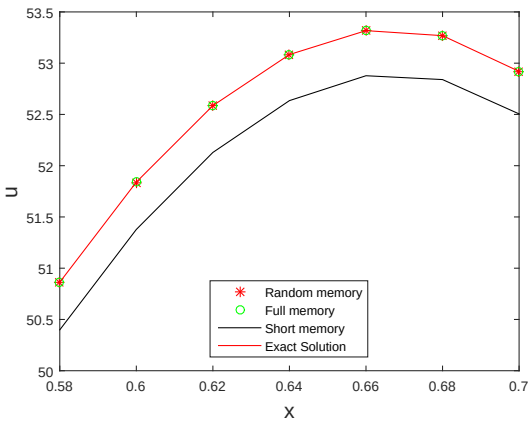

(b) Solutions of (12) at $t = 5$ for $0.58 \leq x \leq 0.7$.

Figure 5: Exact solutions and numerical solutions of the time fractional reaction-diffusion equations (11) and (12) for short ranges of space variable x.

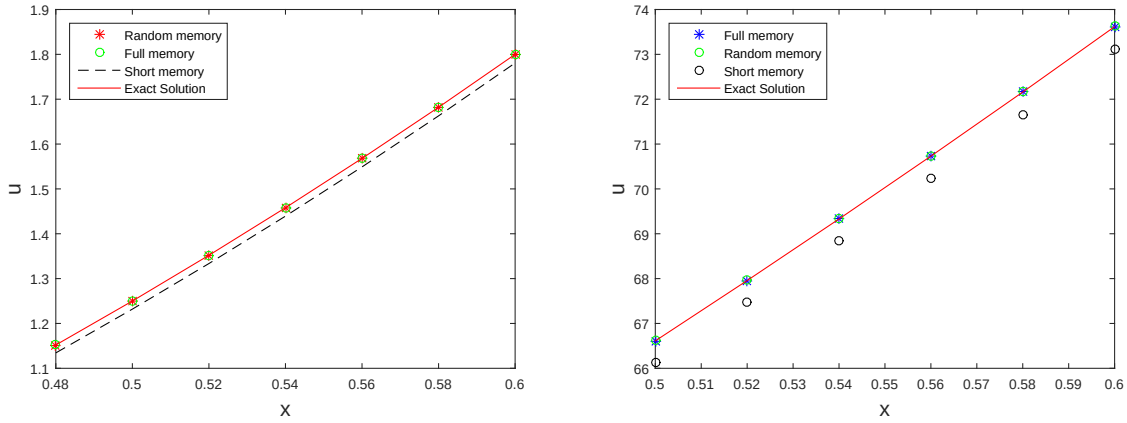

(a) Solutions of (13) at $t = 5$ for $0.48 \leq x \leq 0.6$. (b) Solutions of (14) at $t = 5$, $0.48 \leq x \leq 0.6$

Figure 6: Exact solution and numerical solutions of the time fractional reaction-diffusion equation (13) and (14) for short ranges of space variable x.

Figures 4, 5, and 6 show the solutions of the TFRDEs (11)-(14) on space interval $0 \leq x \leq 1$ and short space intervals respectively. For these numerical simulations, $\Delta t = 0.0005$, $\Delta x = 0.02$, $L = 1$ and $\gamma = 0.9$, percentage memory length $(PML) = 20$ in SI-SMM and $\alpha = 3$, $M = 100$ in SI-EDRMM). Solutions of (14) are relevant to $y = 0.5$. Slight differences between exact solutions and solutions obtained by three numerical schemes are invisible in the plots of full range $0 \leq x \leq 1$ (Figure 4). But these slight differences are visible in the plots of short ranges of space variable x (Figures 5 and 6).

Comparison of numerical schemes

In this section comparison of CPU time (computation time (CT)) and numerical errors of the numerical schemes SI-FMM, SI-SMM, and SI-EDRMM are presented. Numerical errors are compared using Mean Square Error (MSE) between numerical solutions and exact solutions of the considered models. To do this comparison, we define the term "percentage decrease of computational time (PD-CT)" of the numerical scheme SI-SMM as follows

$$\text{PD-CT of SI-SMM} = \frac{\text{CT of SI-FMM} - \text{CT of SI-SMM}}{\text{CT of SI-FMM}} 100\%.$$

PD-CT of SI-EDRMM can be defined in a similar manner. Table 1 shows the CT spent to integrate equations (11), (12),(13) and (14) up to $t = 5$ by the numerical schemes SI-FMM, SI-SMM (for $PML = 20$), SI-EDRMM (for $\alpha = 3$, $M = 100$) and corresponding PD-CT. According to these data, the CT of SI-EDRMM is less than that of SI-SMM and SI-FMM. Also, PD-CT of SI-SMM and SI-EDRMM are approximately 65 and 70 respectively for the TFRDEs (11)-(13) and those values for (14) are approximately 50 and 60 respectively. Therefore, the computational cost of the proposed method has been dropped to more than 60 percent and it is a good performance and successfully faces the challenge of the computational cost of TFRDEs. Table 2 shows the MSE between exact solutions and numerical solutions at $t = 5$ of the above four TFRDEs obtained by the numerical schemes SI-FMM, SI-SMM, and SI-EDRMM. The MSE of SI-EDRMM is less than that of SI-SMM. Therefore, the proposed numerical scheme, SI-EDRMM, is more accurate and efficient than SI-SMM.

Table 1: CT (in seconds) spent to integrate (11), (12), (13) and (14) up to $t = 5$ by SI-FMM, SI-SMM and SI-EDRMM when $\Delta t = 0.0005$, $\Delta x = 0.02$, $L = 1$, $\gamma = 0.9$, ($PML = 20$ in SI-SMM and $\alpha = 3$, $M = 100$ in SI-EDRMM) and corresponding PD-CT values.

	CT			Percentage decrease of CT	
TFRDE	SI-FMM	SI-SMM	SI-EDRMM	SI-SMM	SI-EDRMM
(11)	137.7898	47.1847	37.5596	65.75603	72.74138
(12)	132.4256	46.9760	37.5890	64.5265	71.6150
(13)	128.3693	44.8422	37.7369	65.06782	70.60286
(14)	217.2794	102.5300	84.0766	52.81191	61.30485

Table 2: Mean square error between exact solutions and numerical solutions of the TFRDEs (11), (12), (13) and (14) at $t = 5$ obtained by the numerical schemes SI-FMM, SI-SMM, and SI-EDRMM when $\Delta t = 0.0005$, $\Delta x = 0.02$, $L = 1$, $\gamma = 0.9$, ($PML = 20$ in SI-SMM and $\alpha = 3$ and $M = 100$ in SI-EDRMM).

	MSE		
TFRDE	SI-FMM	SI-SMM	SI-EDRMM
(11)	4.2569×10^{-08}	0.0123	4.2869×10^{-06}
(12)	2.6898×10^{-09}	0.0118	3.5075×10^{-06}
(13)	1.7036×10^{-09}	2.6144×10^{-05}	7.6338×10^{-09}
(14)	6.4782×10^{-08}	0.0077	1.7931×10^{-05}

Table 3: Variation of CT (in seconds) against α of the scheme SI-EDRMM when it applies to simulate models (11), (12), (13) and (14) up to time $t = 5$. ($\Delta t = 0.0005$, $\Delta x = 0.02$ and $M = 100$, $\gamma = 0.9$).

	CT			
α	TFRDE 1	TFRDE 2	TFRDE 3	TFRDE 4
1	127.3680	128.0008	129.5068	191.9183
2	68.8961	68.2440	67.9349	123.7108
3	37.5596	37.5890	37.7369	84.0766
4	24.1688	24.2491	24.4602	66.5762
5	17.1975	17.3299	17.5972	56.7681
6	13.0471	12.5416	13.2837	50.7292

Tables 3 and 4 show the variation of CT and MSE between exact solutions and numerical solutions of the TFRDEs (11), (12), (13) and (14) at $t = 5$ obtained by SI-EDRMM method at different levels of α respectively. We can observe that CT of each model decreases as α increases and MSE is least at $\alpha = 3$ for all four TFRDEs. Therefore, the case $\alpha = 3$ of the SI-EDRMM is more efficient and accurate for these models and the case $\alpha = 3$ can be used for long time integration of these models.

Table 4: Variation of MSE between exact solutions and numerical solutions at time $t = 5$ against α of the SI-EDRMM when it applies to simulate models (11), (12), (13) and (14) ($\Delta t = 0.0005$, $\Delta x = 0.02$, $\gamma = 0.9$ and $M = 100$).

	MSE of TFRDE			
α	(11)	(12)	(13)	(14)
1	4.4946×10^{-05}	7.2598×10^{-05}	1.3503×10^{-07}	8.6866×10^{-05}
2	9.4744×10^{-05}	7.6337×10^{-05}	3.7272×10^{-08}	2.0793×10^{-05}
3	4.2869×10^{-06}	3.5075×10^{-06}	7.6338×10^{-09}	1.7931×10^{-05}
4	6.0004×10^{-04}	9.2545×10^{-04}	2.2156×10^{-06}	2.8102×10^{-04}
5	0.0056	0.0061	9.8472×10^{-05}	0.0036
6	0.0290	0.0257	8.7491×10^{-05}	0.0184

Numerical experiments for simulations on large time intervals

CT and MSE corresponding to integration of TFRDEs (11), (12) and (13) for large time (T=200) by the numerical schemes SI-FMM, SI-SMM, and SI-EDRMM are shown in Tables 5 and 6 respectively. These data confirm that if the proposed method SI-EDRMM is used then computational cost reduces approximately 70 percent for the large-time integrations also.

Table 5: CT (in seconds) spent to integrate (11), (12), (13) and (14) up to $T = 200$ by SI-FMM, SI-SMM and SI-EDRMM when, $\Delta x = 0.02$, $\Delta t = 0.0005$, $L = 1$ and $\gamma = 0.8$, ($PML = 20$ in SI-SMM and $\alpha = 3$, $M = 100$ in SI-EDRMM).

	CT			Percentage decrease of CT	
TFRDE	SI-FMM	SI-SMM	SI-EDRMM	SI-SMM	SI-EDRMM
(11)	551.3747	193.8450	149.1851	64.84333	72.94306
(12)	549.6185	186.1952	146.7626	66.12283	73.29737
(13)	12784.0	4704.7	3794.0	63.19853	70.32228

To compare the accuracy of SI-SMM and SI-EDRMM against SI-FMM, we compare mean square error relative to the exact solution of each numerical scheme. Mean square error relative to the exact solution of SI-FMM (RMSE_E(SI-FMM)) as follows.

$$\text{RMSE}_E(\text{SI-FMM}) = \frac{\text{MSE}(S_{SI-FMM} - S_E)}{||S_E||},$$

where S_{SI-FMM} and S_E are the solution at $T = 200$ obtained by SI-FMM and exact solution respectively. RMSE_E(SI-EDRMM) and RMSE_E(SI-SMM)can be defined in a similar manner. Table 6 shows the mean square errors of the numerical sachems. It can be observed that the relative mean square error of EDRMM is less than that of SMM.

Table 6: Relative mean square error between exact solutions and numerical solutions of the models (11), (12), (13) and (14) at $T = 200$ obtained by the numerical schemes SI-FMM, SI-SMM ($PML = 20$) and SI-EDRMM ($\alpha = 3$ and $M = 100$). $\Delta x = 0.02$, $L = 1$ and $\gamma = 0.8$, $\Delta t = 0.0005$ for TFRDEs (11), (12) and $\Delta t = 0.002$ for (13).

	RMSE_E		
TFRDE	SI-FMM	SI-SMM	SI-EDRMM
(11)	8.3800×10^{-08}	6.8971×10^{-04}	5.7845×10^{-06}
(12)	7.8361×10^{-12}	4.8271×10^{-04}	6.4764×10^{-07}
(13)	8.2416×10^{-10}	2.6203×10^{-09}	2.0417×10^{-09}

Simulation of a time-fractional reaction-diffusion system

In this section, a time fractional reaction-diffusion system that forms spatial-temporal patterns is simulated using the proposed three numerical schemes, and their performance is discussed. The analytical solution of this system is unknown. Consider the following time fractional reaction-diffusion system that appears in Somathilake & Burrage (2021).

$$\begin{aligned} \frac{\partial^\gamma u}{\partial t^\gamma} &= \Delta u + 1 - u - \beta^2 u v^2, \quad (x,y) \in \Omega \subset \mathbb{R}^2, \quad 0 \le t \le T, \\ \frac{\partial^\gamma v}{\partial t^\gamma} &= d\Delta v - \lambda v + \beta^2 u v^2, \quad (x,y) \in \Omega \subset \mathbb{R}^2, \quad 0 \le t \le T, \end{aligned} \tag{15}$$

subject to homogeneous Neumann boundary conditions:

$$\left.\begin{aligned} \nabla u.\mathbf{n} = 0, \quad x \in \partial\Omega \\ \nabla v.\mathbf{n} = 0, \quad x \in \partial\Omega \end{aligned}\right\}. \tag{16}$$

The pattern formation parameter region of the model is explained in the same paper. This model is simulated on the domain $\Omega = (1,2) \times (1,2)$ up to time $T = 20$ using initial conditions as a small perturbation of the equilibrium state of the model relevant to the parameter values $\beta = 7.75$, $\lambda = 3.5$, $\gamma = 0.9$, $d = 0.005$, which lie in the pattern formation parameter region. Isosurfaces of the numerical solutions obtained by three numerical schemes are shown in Figure 7. In these simulations, grid sizes are chosen as $\Delta x = \Delta y = 0.05$, $\Delta t = 0.001$. Also, $\alpha = 3$, $M = 200$ for SI-EDDRM and PML=10 for SI-SMM.

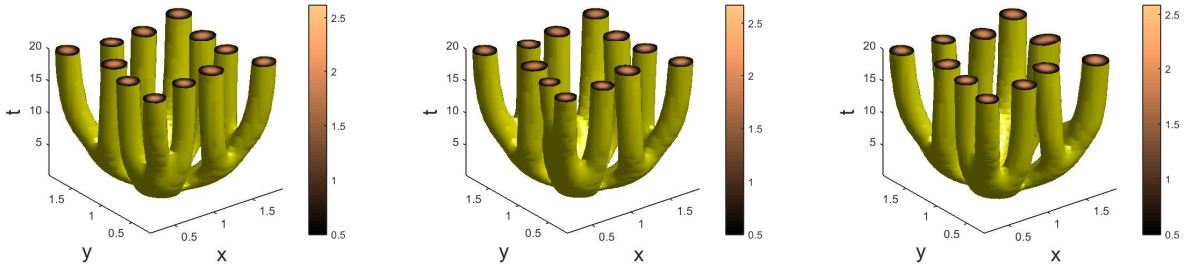

(a) For SI-FMM scheme. (b) For SI-EDRMM scheme (c) For SI-SMM scheme

Figure 7: Isosurfaces of numerical solutions $v(x,y,t)$ for numerical schemes SI-FMM ($PML = 20$) , SI-EDRMM ($\alpha = 3$ and $M = 100$) and SI-SMM for the parameter values $\lambda = 3.5$, $\beta = 7.75$, $d = 0.005$ and $\gamma = 0.9$.

Numerical solutions obtained by three numerical schemes are almost the same. To compare the numerical sachems SI-SMM and EI-EDRMM we define the mean square error of the solution of the last time step relative to the solution obtained by SI-FMM. Define the relative mean square error of SI-SMM (RMSE_{FMM}(SI-SMM)) as follows.

$$\text{RMSE}_{FMM}(\text{SI-SMM}) = \frac{\text{MSE}(S_{SI-FMM} - S_{SI-SMM})}{||S_{SI-FMM}||},$$

where S_{SI-FMM} and S_{SI-SMM} denote the solutions obtained by SI-FMM and SI-SMM respectively. (RMSE_{FMM}(SI-EDRMM) can be defined in a similar manner.

Table 7: RMSE and CT of the numerical schemes in simulating the system (15).

Numerical scheme	RMSE_{FMM}	CT	Percentage decrease of CT
SI-FMM	-	1612.1	-
SI-SMM	15.08497×10^{-5}	951.3	41
SI-EDRMM	2.83664×10^{-5}	757.4	53

Also, according to the data in Table 7, the computational cost of SI-EDRMM is less than that of SI-FMM and SI-SMM, and the relative mean square error of EDRMM is less than that of SI-SMM. Therefore, SI-EDRMM is more efficient than SI-FMM and SI-SMM and is more accurate than SI-SMM in simulating the above system of TFRDEs for the chosen set of parameters.

CONCLUSION

In simulating TFRDEs, large systems of TFDEs have to be solved. As such, numerical integration of time-fractional reaction-diffusion equations is computationally expensive as computational cost mainly depends on the number of vector summations over the considered memory points in the past at each time step. Reducing computation cost is the main challenge in the numerical integration of TFRDEs. Applying well-established memory selection methods FMM and SMM for integration of TFRDEs is very difficult due to the high computational cost and uncontrollable error respectively. This paper compares the memory selection method, EDRMM proposed by Somathilake (2020), FMM, and SMM in time integration of TFRDEs. For this, the author suggests three

semi-implicit numerical schemes SI-EDRMM, SI-FMM, and SI-SMM based on three memory selection methods EDRMM, FMM, and SMM respectively. These three numerical schemes are compared by simulating four TFRDEs whose exact solutions are known and one system of TFRDEs whose exact solution is unknown.

The accuracy and efficiency of SI-EDRMM can be controlled by varying the parameter values α and M of this method. It is observed that the most accurate solutions of the considered models are given at $\alpha = 3$ of SI-EDRMM. The computational cost of SI-EDRMM (for $\alpha = 3$) is less than that of SI-FMM and SI-SMM (for PML=20). Therefore, SI-EDRMM is more efficient than SI-FMM and SI-SMM.

The MSE between exact solutions and numerical solutions obtained by SI-EDRMM ($\alpha = 3$) is less than that of SI-SMM. That is SI-EDRMM ($\alpha = 3$) is more accurate than the SI-SMM (PML=20). Therefore, SI-EDRMM is better for the numerical integration of chosen TFRDEs, because of its adequate accuracy and low computational cost. Similar results were observed when simulating the chosen system of TFRDEs.

REFERENCES

Abdelouahab M.-S. & Hamri N.-E. (2016). The Grünwald–Letnikov fractional-order derivative with fixed memory length. *Mediterranean Journal of Mathematics* **13**(2): 557–572.DOI: https://doi.org/10.1007/s00009-015-0525-3.

Baeumer B., Kovács M. & Meerschaert M. M. (2008). Numerical solutions for fractional reaction–diffusion equations. *Computers & Mathematics with Applications* **55**(10): 2212–2226.DOI://doi.org/10.1016/j.camwa.2007.11.012.

Caballero J., Harjani, J. & Sadarangani K. (2011). Existence and uniqueness of positive solution for a boundary value problem of fractional order. In *Abstract and Applied Analysis*, volume **2011** Hindawi. Article ID 165641, 12 pages.
DOI: http://:10.1155/2011/165641.

Deng J., Zhao L. & Wu Y. (2016). Fast predictor-corrector approach for the tempered fractional differential equations. *Numerical Algorithms*, 1–38.
DOI: https://doi: 10.1007/s11075-016-0169-9.

Deng W. (2007). Short memory principle and a predictor–corrector approach for fractional differential equations. *Journal of Computational and Applied Mathematics* **206**(1): 174–188
.DOI: https://doi:10.1016/j.cam.2006.06.008.

Deng W. & Li C. (2012). *Numerical schemes for fractional ordinary differential equations*. INTECH Open Access Publisher.

Diethelm K., Ford N. J. & Freed A. D. (2002). A predictor-corrector approach for the numerical solution of fractional differential equations. *Nonlinear Dynamics*, **29**(1): 3–22.

El-Sayed A. & El-Maghrabi E. (2008). Stability of a monotonic solution of a non-autonomous multidimensional delay differential equation of arbitrary (fractional) order. *Electronic Journal of Qualitative Theory of Differential Equations*, **2008**(16): 1–9.

Gafiychuk V. & Datsko B. (2010). Mathematical modeling of different types of instabilities in time fractional reaction-diffusion systems. *Computers & Mathematics with Applications* **59**(3): 1101–1107.DOI: https://doi:10.1016/j.camwa.2009.05.013.

Karatay, İ., Bayramoğlu Ş. R., & Şahin A. (2011). Implicit diffe rence approximation for the time fractional heat equation with the nonlocal condition. *Applied Numerical Mathematics*, **61**(12): 1281–1288.DOI: https://doi.org/10.1016/j.apnum.2011.08.007.

Khan N. A., Khan N.-U., Ara A. & Jamil M. (2012). Approximate analytical solutions of fractional reaction-diffusion equations. *Journal of King Saud University-Science* **24**(2): 111–118.
DOI: http://:10.1016/j.jksus.2010.07.021.

Lakshmikantham, V. & Vatsala, A. (2008). Basic theory of fractional differential equations. *Nonlinear Analysis: Theory, Methods & Applications*, **69**(8), 2677–2682.
DOI: https://doi:10.1016/j.na.2007.08.042.

Murio D. A. (2008). Implicit finite difference approximation for time fractional diffusion equations. *Computers & Mathematics with Applications* **56**(4), 1138–1145.
DOI: http://10.1016/j.camwa.2008.02.015.

Podlubny & Igor (1999). *Fractional Differential Equations, an introduction to fractional derivatives, fractional differential equations, to methods of their solution and some of their applications*. Mathematics in science and engineering, 198. San Diego : Academic Press.

Rida S., El-Sayed, A., & Arafa, A. (2010). On the solutions of time-fractional reaction–diffusion equations. *Communications in Nonlinear Science and Numerical Simulation* **15**(12), 3847–3854.
DOI: https://doi:10.1016/j.cnsns.2010.02.007.

Scherer R., Kalla, S. L., Tang, Y., & Huang, J. The grünwald–letnikov method for fractional differential equations. *Computers & Mathematics with Applications* **62**, *number=3, pages=902–917, year=2011, publisher=Elsevier, note=*
DOI: https://doi:10.1016/j.camwa.2011.03.054.

Somathilake, L. W. (2020). An efficient numerical method for fractional ordinary differential equations based on exponentially decreasing random memory on uniform meshes. *Journal of the National Science Foundation of Sri Lanka* **48**(2), 163–174.
DOI: http://dx.doi.org/10.4038/jnsfsr.v48i2.9026.

Somathilake, L. W. & Burrage, K. (2021). Pattern formation in a time fractional reaction–diffusion system. *Journal of Fractional Calculus and Applications*, **12**(1), 9–24. http://math-frac.oreg/Journals/JFCA/.

Xu Y. & He, Z. (2011). The short memory principle for solving abel differential equation of fractional order. *Computers & Mathematics with Applications*, **62**(12), 4796–4805.
DOI: https://doi:10.1016/j.camwa.2011.10.071.

Zheng M., Liu, F., Liu, Q., Burrage, K., & Simpson, M. J. (2017). Numerical solution of the time fractional reaction–diffusion equation with a moving boundary. *Journal of Computational Physics*, **338**, 493–510.
DOI: http://dx.doi.org/10.1016/j.jcp.2017.03.006.

Zhou W.-X., Peng, J.-G., & Chu, Y.-D. (2012). Multiple positive solutions for nonlinear semipositone fractional differential equations. *Discrete Dynamics in Nature and Society*, **2012**. Article ID 850871,10 pages.
DOI: http://doi:10.1155/2012/850871.

Zhuang P. & Liu, F. (2006). Implicit difference approximation for the time fractional diffusion equation. *Journal of Applied Mathematics and Computing*, **22**(3), 87–99.
DOI: https://doi.org/10.1007/BF02832039.